GROWTH AND CHARACTERIZATION OF CdO STRUCTURES FOR SOLAR CELL APPLICATION

MUSTAFA ZAIEN MOHAMMED

UNIVERSITI SAINS MALAYSIA

2015

GROWTH AND CHARACTERIZATION OF CdO STRUCTURES FOR SOLAR CELL APPLICATION

By

MUSTAFA ZAIEN MOHAMMED

Thesis submitted in fulfillment of the requirements for the degree of Doctor of Philosophy

January 2015

DEDICATION

To my family and all the people who have supported me during my life.

ACKNOWLEDGMENTS

First and foremost, I would like to thank Allah for granting me health and patience to finish this research.

I owe the greatest gratitude to my main supervisor, Dr. Naser M. Ahmed, and my co-supervisor, Prof. Dr. Zainuriah Hassan, for their scholarly guidance and dedicated time and support throughout the course of this study.

I also owe gratitude to my father for his support and encouragement. My appreciation goes to my wife and children for their patience and love, which served as my bulwark during the conduct of this research.

Much of this work would have been virtually impossible without the technical support offered by our helpful laboratory assistants at the School of Physics, Universiti Sains Malaysia.

Eventually, I would like to thank all my friends and colleagues who supported me and helped me at the School of Physics, Universiti Sains Malaysia.

TABLE OF CONTENTS

LIST OF TABLES

LIST OF FIGURES

LIST OF SYMBOLS

a, b, and *c*	Lattice parameters
C	The lattice constant of the strained lattice of crystalline CdO
C_o	The standard lattice constant of the crystalline CdO
D	Average crystallite size
d	The spacing between adjacent planes
E_g	Energy band gap
E_C	The conduction band energy level
E_V	The valence band energy level
E_F	Fermi energy
h	Plank's constant
hkl	Miller indices
hv	The energy of the photon
I	Current
I_m	Maximum current
I_{sc}	Short circuit current
I-V	Current-voltage
J	Current density
J_{sc}	Short circuit current density
J-V	Current density-voltage
K	Boltzmann's constant

m_e^*	Electron effective mass
m_h^*	Hole effective masses
$N(E)$	Density of states
n	Carrier concentration
P_m	Maximum power output
P_{in}	Incident solar power
R	Particle radius
R_S	Sheet resistance
V	Voltage
V_m	Maximum voltage
V_{oc}	Open circuit voltage
μ_H	Hall mobility
η	Conversion efficiency
ρ	Electrical resistivity
λ	The wavelength
α	The absorption coefficient
$\mathcal{E}_{zz}$	Strain

LIST OF ABBREVIATIONS

AFM	Atomic force microscope
a.u.	Arbitrary unit
CdO	Cadmium oxide
EDX	Energy dispersive X-ray
e-h	Electron–hole
FF	Fill factor
FWHM	Full width at half maximum
He-Cd	Helium cadmium
NBE	Near-band-edge
PL	Photoluminescence
PV	Photovoltaic
RCA	Radio Corporation of America
SEM	Scanning electron microscopy
sccm	Standard cubic centimeters per minute
SVD	Solid–vapor deposition
TCO	Transparent conductive oxide
UV/Vis	Ultraviolet / Visible
XRD	X-ray diffraction
2D	Two dimensional
3D	Three dimensional

PERTUMBUHAN DAN KARAKTERISASI STRUKTUR CdO BAGI APLIKASI SEL SOLAR

ABSTRAK

Struktur cadmium okside (CdO) yang berbeza berjaya disintesis melalui mendapan pepejal-wap (SVD) bagi serbuk Cd dan CdO dalam relau tiub kuartza mendatar di atas substrat silikon jenis-p pada suhu yang berjulat daripada 1235 K hingga 1400 K dengan aliran argon dan oksigen. Mikroskopi imbasan elektron penskanan (SEM) menunjukkan bahawa morfologi CdO mempamerkan struktur CdO yang berbeza atas substrat Si, iaitu kelopak seperti dendrite, seperti rumput, rod mikro dan hablur nano, melalui mendapan pepejal-wap tanpa vakum dan pemangkin di bawah parameter pertumbuhan yang berbeza. Tambahan pula, sifat struktur, optik, dan electrik struktur nano CdO juga dikaji den diselidiki. Struktur nano mempunyai purata saiz hablur daripada 30 nm hingga 35 nm.

SEM juga mempamerkan pelbagai bentuk struktur mikro CdO bergantung pada kedudukan substrat Si daripada bahan sumber (serbuk CdO) dalam relau. Struktur mikro CdO merangkumi rod mikro, kiub mikro dan seperti pek rumput. Sifat struktur dan optic struktur mikro CdO dikaji. Purata saiz hablur berkurangan dengan pertambahan pemalar kekisi apabila jarak substrat daripada bahan sumber semasa pertumbuhan bertambah.

Filem nipis CdO juga diendapkan di atas substrat silikon jenis p dan substrat kaca pada suhu bilik melalui kaedah penyejatan haba bagi serbuk CdO dalam vakum. Corak belauan sinar X (XRD) menunjukkan bahawa struktur CdO yang berbeza adalah

polihablur dengan struktur kiub melalui kaedah kajian ini. Jurang tenaga jalur terus adalah 2.2 eV hingga 2.5 eV.

Pengukuran Hall menunjukkan bahawa filem nipis CdO adalah jenis n. Jurang jalur terus optik semakin berkurangan, sedangkan kekonduksian elektrik dan kepekatan pembawa semakin meningkat selepas penyepuhlindapan pada 500 °C selama 1 jam bagi filem nipis CdO yang dimendapkan pada substrat kaca melalui penyejatan haba dalam vakum.

Kaedah ini digunakan untuk memfabrikasi sel suria n-CdO/p-Si disebabkan darjah kekasarannya yang tinggi dan pantulan efektif yang minimum diperoleh melalui mendapan filem nipis n-CdO pada substrat Si jenis p. Tambahan pula, kecekapan sel suria n-CdO/p-Si adalah 5.51% pada keadaan iluminasi 100 mW/cm^2 melalui kaedah mendapan pepejal-wap, dan 5.92% melalui penyejatan haba dalam kaedah vakum.

GROWTH AND CHARACTERIZATION OF CdO STRUCTURES FOR SOLAR CELL APPLICATION

ABSTRACT

Different structures of cadmium oxide (CdO) were successfully synthesized using a solid-vapor deposition (SVD) for Cd and CdO powders in a horizontal quartz tube furnace on p-type silicon substrates at temperature ranging from 1235 K to 1400 K with argon and oxygen flows. Scanning electron microscopy (SEM) revealed that the CdO morphology exhibited different structures of CdO on Si substrates, such as dendrite-like petals, grass-like, microrods, and nanocrystalline thin films, via solid-vapor deposition without a vacuum and catalyst under different parameters of growth. Moreover, the structural, optical, and electrical properties of structures of CdO were studied and investigated. The structures had an average crystallite size of 30 nm to 35 nm.

SEM also exhibited various shapes of CdO microstructures depending on the position of Si substrates from the source material (CdO powder) in the furnace. The CdO microstructures included microrods, microcubes, and grass packs-like. The structural and optical properties of CdO microstructures were studied. The average crystallite size decreased with an increase in the lattice constant when the distance of the substrates from the source material during growth was increased.

CdO thin films were also deposited on p-type silicon and glass substrates at room temperature using the thermal evaporation method for CdO powder in a vacuum. The X-ray diffraction (XRD) pattern showed that different structures of CdO were polycrystalline in nature with a cubic structure using these methods in this study. Direct band gap energy was 2.2 eV to 2.5 eV.

Hall measurements revealed that the thin films of CdO were of n-type. The optical direct band gap was decreased, whereas electrical conductivity and carrier concentration increased after annealing at 500 °C for 1 h for CdO thin films were deposited on glass substrates using thermal evaporation in vacuum.

These methods were used to fabricate n-CdO/p-Si solar cells due to the high degree of roughness and the minimum effective reflectance obtained by deposition of n-CdO thin films on p-type Si substrates. Moreover, the solar cell efficiency of the n-CdO/p-Si was 5.51% under 100 mW/cm^2 illumination conditions via the solid-vapor deposition method while it was 5.92% using the thermal evaporation in a vacuum method.

CHAPTER 1

INTRODUCTION

1.1 Overview

The physics of thin films is an important branch of solid state physics. The term thin film is used to describe a layer or layers of material's atoms with a thickness not exceeding 1μm [1, 2]. Moreover, thin films significantly influence studies of the physical properties of materials that cannot be studied in their bulk phases [1]. Thin films are used in many modern electronic fields, such as the fields of electronic circuits, photodiodes, optoelectronics, phototransistors, transparent electrodes, gas sensors, and solar cells [2, 3]. The importance of thin films has stimulated the emergence and development of different methods for fabricating such films.

Nanostructured materials are attractive and interesting materials for many optoelectronic applications because of their unique chemical and physical properties, which differ from those of bulk materials or single atoms their distinctive chemical and physical qualities, which varies compared to those of bulk materials or single atoms [4]. The properties of such materials depend on structure type, nature of surface, and dimension, such as nanoparticles, nanocubes, nanorods, nanowires, nanoflowers, nanotubes, and nano-thin films [5]. The nanostructured materials have dimensions between in 1 nm to 100 nm [6]. Many methods have been adopted to synthesize micro- and nano-thin films, such as spray pyrolysis, sputtering, chemical bath deposition, sol-gel method, vapor–liquid–solid method (VLS), vapor transport or solid–vapor deposition (SVD), and thermal evaporation in a vacuum [6].

Energy is the most important problem facing mankind. Solar energy is a renewable energy source that offers a potentially endless energy supply that can meet the electricity demands of the entire world [7]. Therefore, researchers have studied and fabricated heterojunctions for solar cells from micro- and nano-materials. A solar cell is a device that converts solar energy into electrical energy [8]. This phenomenon is called the photovoltaic (PV) effect. This technology is characterized by simplicity because it involves only the application of sunlight to a crystal surface to produce electricity. This technology is also free of pollution and noise and has low economic cost [9].

The compounds of II–VI semiconductors represent some of the highly used compounds in the manufacture of optoelectronic devices, such as solar cells, because these semiconductors have high efficiency in generating electron–hole pairs (i.e., high quantity efficiency) and high absorption coefficient with direct band gap energy [10-12]. Among the II–VI semiconductors, cadmium oxide (CdO) is the most significant transparent conductive oxides (TCOs) [13, 14]. Technological interest in TCO materials has grown tremendously after Bädeker prepared CdO films by thermally oxidizing sputtered cadmium in 1907 [15, 16]. CdO exhibits intrinsic features that include an intermediate direct band gap ranging from 2.2 eV to 2.5 eV [17], high electrical conductivity (even without doping), and high carrier concentration at room temperature [18, 19]. Thus, different structures of CdO (micro- and nano) are now widely used in various physical applications, such as electronic and optoelectronic devices [8, 13]. CdO are also commonly applied as n-type window layers (photoconductive material) in the thin films of solar cells because of its high transparency in the visible region of the solar spectrum [20, 21].

Vapor transport (SVD) without a catalyst and thermal evaporation in a vacuum are the most attractive methods to synthesize and grow different CdO structures because of their low cost and simplicity. The products of these methods depend on parameters of synthesis and growth, such as reaction temperature, the gas flow rate, and the position of the substrate from the source material in the furnace. CdO has many applications depending on the structure shape of CdO (microstructure or nanostructure). Vapor transport and thermal evaporation are used to fabricate heterojunctions for solar cells, such as n-CdO/p-Si has been fabricated from CdO micro- or nano-thin film deposited on Si substrates because of the high crystallinity of these thin films and their minimum light reflection with superior light trapping in the visible region. These properties increase the efficiency of solar cells [13, 8].

Currently, micro- and nano-structured materials are not only in the forefront of the hottest studies on fundamental materials, but are also gradually being used in daily life. However, the increased development in electronic technology has brought about the need for better understanding of the optical and electrical properties of CdO microstructures and nanostructures, which are used to fabricate numerous electronic products.

1.2 Problem Statement

Different structures (micro- and nano) of CdO can be widely prepared using vapor transport with gas flow and thermal evaporation in vacuum methods. In this study, vapor transport (SVD) was used to synthesize thin films and other CdO structures, such as nanocrystalline thin films, microcubes, and microrods, in a tube of a small furnace without a vacuum and catalyst depending on the different parameters of synthesis.

However, this method has its disadvantages. For example, the method requires high temperature to evaporate the source material (CdO powder). Because of the requirement of high melting point, the method cannot determine the thickness of thin films used in the fabrication of solar cells. Furnace setup also involves several problems, such as the small diameter of the furnace tube. These drawbacks create difficulties in controlling the parameters of synthesis and growth of CdO. Thus, the preparation process needs to be skillfully done, and the structural, optical, and electrical properties are improved in the preparation of CdO/Si samples, such as thin films have good homogeneous, high absorption in the visible region, high electrical conductivity, and high carrier concentration so as to fabricate highly efficient solar cells. In addition, thermal evaporation in a vacuum was used to deposit CdO thin films. Few studies have synthesized different structures of CdO and fabricated CdO/Si solar cells using these methods. Thus, more studies should investigate the effect of the parameters of the synthesis and growth of CdO on its structural, optical, and electrical properties via simple methods that lower the cost of fabrication of optoelectronic devices, specifically solar cells.

1.3 Research Objectives

The main objectives of this study are to:

a) Synthesize and grow different structures (micro-and nano) of CdO on Si substrates via SVD under different parameters of growth, and study their structural, optical, and electrical properties.

b) Deposit CdO thin films on glass substrates via thermal evaporation in vacuum and study the effects of annealing on their structural, optical, and electrical properties.

c) Fabricate n-CdO/p-Si solar cells using SVD and thermal evaporation in vacuum, and study their electrical (I-V) properties.

1.4 Originality of this Research

The originality of this study lies in the following aspects:

a) Dendrite-like petals of CdO microstructures were grown by SVD without a catalyst.
b) CdO/Si heterojunction was fabricated as a solar cell via the SVD method.
c) Different structures of CdO microstructures were grown using SVD depending on the position of Si substrates from the source material. The effect of this growth parameter on the morphological properties of CdO was investigated.

1.5 Scope of Study

Using the SVD method, varying structures of CdO were grown on Si substrates, and their structural, optical, and electrical properties were investigated to be used in optoelectronics and electronics applications. The prepared thin films of CdO were used to fabricate a solar cell. For comparison, a CdO/Si solar cell was also fabricated by thermal evaporation in a vacuum to enhance performance.

1.6 Outline of the Thesis

The contents of this thesis are organized as follows:

Chapter 1 provides a concise synopsis of the research subject. **Chapter 2** reviews related literature on synthesis of CdO thin films, effects of annealing on their properties, the

growth of CdO different structures, and their applications in solar cells. The physical and chemical properties of CdO are explained. This chapter also discusses theoretical concepts of semiconductors, nanostructured material properties, and energy bands in heterojunction as well as the fundamentals of solar cell with its parameters. **Chapter 3** describes synthesis equipments and discusses the principles of the tools and parameters used to characterize the optical, structural, and the electrical attributes of different structures grown, prepared thin films, and solar cells. **Chapter 4** contains the methodology and explains the synthesis methods of CdO structures. This chapter also describes the synthesis of different microstructures, nanostructures, and thin films of CdO with the effects of annealing. In addition, the chapter details the fabrication of solar cells using SVD and thermal evaporation in a vacuum. **Chapter 5** presents the results of growth of CdO different structures (micro- and nano) using SVD under different parameters of growth and their structural, optical, and electrical properties are studied. In addition, CdO/Si solar cell is fabricated by the same method and its electrical (I-V) properties are investigated in this chapter. **Chapter 6** presents the effects of annealing on the structural, optical, and electrical properties of CdO thin films deposited on glass substrates via thermal evaporation in vacuum. In this chapter, CdO/Si solar cell is also fabricated by thermal evaporation and its morphological, structural, optical, and electrical properties are studied. **Chapter 7** includes the concluding part of the thesis as well as recommendations for future works.

CHAPTER 2

LITERATURE REVIEW AND THEORETICAL CONCEPTS

2.1 Introduction

This chapter presents a literature review on CdO thin film synthesis, effects of annealing on their properties, the growth of CdO different structures, and their applications in solar cells. Theoretical concepts of semiconductors, nanostructured material properties, and energy bands in heterojunction as well as fundamental concepts and parameters of solar cell are discussed.

2.2 Synthesis of CdO Thin Films

Over the years, TCO materials have drawn enormous technological attention, beginning with the study by Bädeker (1907), where he prepared CdO thin films for the first time by thermally oxidizing sputtered cadmium [22]. Singh and Dayal (1969) measured the lattice constants and thermal expansion coefficients of CdO at elevated temperatures ranging from 32 to 732°C [23]. Benedict and Look (1970) examined the electrical properties of polycrystalline CdO at temperatures ranging from 1.4 to 300K. These studies discovered that majority of charge carriers are electrons, indicating that the material was of n-type and the concentration of the carriers was based on different temperatures [24]. Furthermore, Call *et al.*, (1980) [25] investigated the structural properties of ZnO, CdO, and CdS films using Miller indices, and carried out a comparative analysis with values of the bulk form to show the deposition of the equilibrium phase. In addition, Benko and Koffyberg (1986) measured the quantum

efficiency (η) of CdO films in the range (1-4 eV). The plotted η curve showed an indirect relationship with the optical absorption coefficient (α), although the direct band gap energy (2.18 eV) was in conformity with previous studies [26]. Several methods have been applied to fabricate CdO films at different temperatures. Dantus *et al.* [27] prepared CdO thin films on glass substrates by thermally oxidizing vacuum evaporated cadmium (Cd) thin films at 650 K. The electrical conductivity property of the CdO thin films was found to be approximately 5×10 to 5×10^{4} $\Omega^{-1}cm^{-1}$ at room temperature, while the optical direct band gap varied between 2.20 and 2.22 eV. Dantus *et al.* [28] also synthesized CdO thin films via thermal evaporation of CdO powder under vacuum with source temperature of 900 K, the electronic transport mechanism of thin films was elucidated based on the Seto's model, while values of optical band gap were been measured from the absorption spectra. Furthermore, Suhail *et al.* [29] examined the impact of temperature on the structure and optical attributes of CdO films synthesized by subjecting CdO powder to thermal evaporation in a vacuum. They noted that the direct band gap decreased with rising substrate temperature as a result of the enlarged grain size and decreasing defect density. Mahaboob *et al.* [30] studied the structural, optical and morphological properties of CdO thin films deposited on glass substrates. XRD patterns showed the thin films are polycrystalline in nature with preferential orientation along (111) plane. Hassan *et al.* prepared CdO thin films on glass substrates using different substrate (deposition) temperatures. Based on the calculated energy gaps of thin films, the study showed that sheet resistance decreased with increasing deposition temperature possibly due to the increase in free carrier concentration [31]. Sankarasubramanian *et al.,*

[32] also determined the average optical transmittance, resistivity, mobility, and carrier concentration of CdO thin films deposited on glass substrates.

2.3 Effects of Annealing on the Characteristics of CdO Thin Films

There are few studies published on the effects of annealing on the characteristics of CdO thin films. Eze synthesized CdO thin films on glass substrates using a modified reactive thermal evaporation technique with annealing treatment at 250-300 °C in oxygen. The identity of the resulting CdO was established with X-ray diffraction, while electrical and optical measurements showed that the thin films were n-type and the band gap was 2.45 eV direct [33]. A study by Vigil *et al.*, [34] discovered that increase in crystallite size and electron mobility due to augmented annealing time reduces the band gap energy, lattice constants and electrical resistivity of CdO thin films. Dakhel and Henari [35] prepared CdO films on a glass substrate at room temperature via thermal evaporation in the absence of air. X-ray diffraction (XRD) showed the films are characterized by a cubic system with lattice parameter of a = 4.69±0.02 Å. The optical and electrical measurements of the thin films, obtained at varying annealing temperatures, showed that average grain size increase with increase in temperature of annealing. Ismail [36] observed that the direct band gap, lattice constant and electrical resistivity of annealed films decreased as annealing time increased. The resistivity of films reached a minimum value of 6×10^{-4} Ωcm and then gradually saturates with increasing annealing times. A study by Salunkhe *et al.*, on the impact of annealing effects on the properties of CdO thin films showed that electrical resistivity and the energy band gap decreased after annealing due to the decrease in defect levels [37]. Gokul *et al.* also

evaluated the changes in intrinsic properties of CdO thin films as a result of annealing at 250-450°C for duration of 2h. Their study deduced certain observations: transmittance decreases with rising annealing temperature; the estimated band gap energy ranges between 2.24 and 2.44eV; Hall effect measurement increases in carrier concentration and resistivity decreases with increasing annealing temperature [38]. In addition, a study by Azizar *et al.,* [39] on the effects of annealing on CdO thin films properties found that grain size, carrier density, and mobility increased with annealing, while the direct and indirect optical band gaps decreased with increasing annealing temperature.

2.4 Synthesis and Growth of Different CdO Structures

Several different structures of CdO (nano- and micro) have been synthesized using vapor transport process in the absence of vacuum and catalyst by means of solid-vapor deposition, or in the presence of catalyst via vapor-liquid-solid (VLS) deposition. Pan *et al.*, [40] synthesized nanobelts of semiconductor oxides of zinc, tin, indium, cadmium, and gallium by basically evaporating the metal oxide powders at 1000 °C in the absence of catalyst. They observed that the as-synthesized oxide nanobelts were pure, structurally homogeneous, monocrystalline, and lacked defects and dislocations. Liu *et al.* [41] synthesized CdO nanoneedles via the vapor transport (VLS) of Cd vapor along with trace amount of oxygen in an argon flow to the Si/SiO_2 substrates zone, and subsequently heated to 850-900 °C for 30 min using gold as a catalyst. The Cd vapor was generated from Cd metal at 350 °C. After investigating their inherent electronic, optoelectronic, and chemical sensing properties, the study showed that the nanoneedles were monocrystalline of large diameters that increased with time. Wang also synthesized

nanobelts of CdO via the solid-vapor process of CdO powder at 1000 °C under argon flow [42]. The surface morphology of CdO was characterized by growth sheets of different shapes along with the nanobelts. The sheets exhibited sizes of up to several tens of micrometers, while the lengths of the nanobelts were less than 100 μm with widths ranging from 100 to 500 nm. Kou and Huang [43] synthesized necklace-like CdO nanowires on Si substrates using a VLS growth mechanism for Cd powder in a tube furnace at 500 °C with argon and oxygen flows. The study showed that the nanowires exhibited diameters ranging from few tens of nanometers to 30-50 μm as a result of a long duration of reaction (2 h). They also observed an emission peak (2.25 eV) centered at 550 nm of photoluminescence spectrum, attributable to the presence of CdO nanowires. A similar study by Srivastava *et al.*, [44] demonstrated the growth of a range of nano- and micro CdO structures (tubular, cylindrical, horse-shoe, cuboids, and nanorods) via the metal-catalyst free-vapor phase deposition (solid-vapor) of Cd granules in furnace under atmospheric pressure at high temperature of 1273 K. A contemporary work by Lu *et al.*, [45] utilized the simple thermal evaporation under argon and air flow to prepare CdO nanotubes (NTs) from Cd powder at 500 °C for duration of 30 min in the absence of any catalyst. Their study showed that CdO NTs is characterized by polycrystalline structure, with lengths of over a few tens of micrometers and a mean diameter of 50 nm. Using a similar method but under different conditions, Fan [46] synthesized CdO nanowires and nanotubes on Si substrates at low temperatures with argon and oxygen flows in a horizontal tube furnace system at various distances between the substrates and the evaporation source. The study also synthesized CdO nanowires at 520°C close to the Cd source (4 cm), while nanotubes were grown on a substrate far from

the Cd source (15 cm) at 400°C. XRD analysis showed that the synthesized nanowires and nanotubes exhibit high crystallinity and are characterized by face-centered cubic CdO structures. Furthermore, Ghoshal *et al.* [47] synthesized CdO nano and micro crystals under different temperatures of growth. The study obtained direct and indirect band gap values of 2.52 eV and 1.78 eV respectively. In a study carried out to synthesize CdO nanospheres, Clament *et al.,* [48] derived direct band gap value of 2.52eV from diffused reflectance spectra. The synthesized CdO nanospheres showed good optoelectronic properties. In the process of synthesizing CdO nanoparticles, Anandhan *et al.* [49] observed that energy band gap decreases with increasing reaction temperature, which confirmed the quantum confinement effect of semiconducting CdO nanoparticles. In other related studies, Pavithra *et al.* [50] studied the structural and optical properties of nanocrystalline CdO thin films synthesized on glass substrates. Mohamed *et al.* [51] grew CdO nanowires on Au coated Si and quartz substrates using vapor transport method. The diameters of the nanowires ranged from 30-90 nm with lengths greater than 30μm, while the optical band gap was measured at 2.41 eV.

2.5 CdO Thin Films in Solar Cells Fabrication

The fabrication and development of economical viable solar cells has garnered considerable attention from researchers, particularly CdO because of its intrinsic properties. Several studies investigated the inherent properties of fabricated CdO thin films based on its conversion efficiency, electrical resistivity and electron mobility. Champness *et al.*, [52] fabricated photovoltaic Se-CdO thin film cell via the reactive sputtering of CdO on a crystallized Se film. They detected cell conversion efficiency (η) of approximately 1.7%, which is higher than values associated with commercial selenium

photovoltaic cells. Shih *et al.*, [53] fabricated a semiconductor-insulator-semiconductor photovoltaic structure in the form of CdO-SiO_2-Si by reactively sputtering a layer of n-type CdO on a thin SiO_2 layer thermally grown on a p-type Si substrate. The cell exhibited an estimated air mass (AM) of 1 illumination and conversion efficiency (η) of about 7% based on its photovoltaic features. Sravani *et al.*, [54] fabricated n-CdO/p-CdTe heterojunction solar cell via the electron beam evaporation of CdTe onto CdO films obtained by activated reactive evaporation. Electrical conversion efficiency of about 7.7% was recorded for the cell with specific surface area of 1 cm^2 under a solar input of 85mW/cm^2. Champness and Chan [55] fabricated Se-CdO photovoltaic cell through the sputtering of the CdO layer on Se with an optimized CdO window layer, although in the absence of an optimized assembling grid or antireflection coating. The fabricated Se-CdO photovoltaic cell exhibited a conversion efficiency η of about 2.5% under solar input of 100 mW/cm^2 of solar irradiance, which is higher compared to the conventional selenium cell (0.3%). Similarly, Al-Quraini and Champness [56] fabricated photovoltaic cells ($CuInSe_2$/CdO and $CuInSe_2$/CdS/CdO layer structures), where the CdO window layer of both devices was deposited by sputtering, and CdS interlayer was deposited by a chemical bath method. A conversion efficiency of approximately 6.3% and 6.8% for the first and second kind of cells, respectively. In addition, Ismail and Abdulrazaq [57] used the rapid thermal oxidation (RTO) technique to deposit CdO thin films of 200 nm thickness on p-type monocrystalline Si substrate to produce a solar cell by means of a halogen lamp at 350 °C/45s in static air. The electrical and photovoltaic features of CdO/Si solar cell showed that CdO/Si had electrical resistivity, electron mobility, and η values of 5×10^{-4} Ωcm, 22 cm^2/Vs, and 8.84%, respectively. Similarly, Yahiya [58]

fabricated CdO/Si heterojunction solar cell by vacuum evaporation of CdO thin film with 300 nm thickness onto monocrystalline Si substrate from CdO powder. The photovoltaic properties of the solar cell exhibited a conversion efficiency η of 5.5% at AM1 illumination power density of 93 mW/cm^2. Inpasalini *et al.*, [59] deposited and fabricated p-NiO/n-CdO heterojunction on glass substrate using the spray pyrolysis technique under optimized condition. The analysis of the photovoltaic properties of the solar cell exhibited conversion efficiency, η of 1.34% under an illumination of 50 mW/cm^2.

2.6 Physical and Chemical Properties of CdO

CdO is a compound semiconductor comprising of cadmium and oxygen [13]. CdO is currently used extensively as TCOs in various physical applications [60], particularly in the production of optoelectronic devices such as n-type window layer in thin films for solar cells as a result of its high transparency in the visible region of the solar spectrum [52, 20]. CdO is solid brown in color and exhibit certain intrinsic features such as high density (8150 kg/m^3), high melting point (1500 °C), and molecular weight (128.4 gm/mol) [61]. It is characterized by a cubic crystal structure [NaCl (fcc) type; lattice constant a = 0.4695 nm] with an alternate sequence of Cd and oxygen atoms positioned within a lattice arrangement [62, 63], as shown in Figure 2.1. Furthermore, CdO has a high electrical conductivity (low resistivity), which is a resultant effect of moderate electron mobility and higher carrier concentration arising from native defects of oxygen anionic vacancies and cadmium interstitials [66-68]. CdO also consists of an intermediate direct band gap ranging from 2.2 eV to 2.5 eV as thin films, and 2.5 eV as

bulk [43, 69]. CdO can also be obtained by directly heating cadmium in air to temperature as high as 900 °C [26].

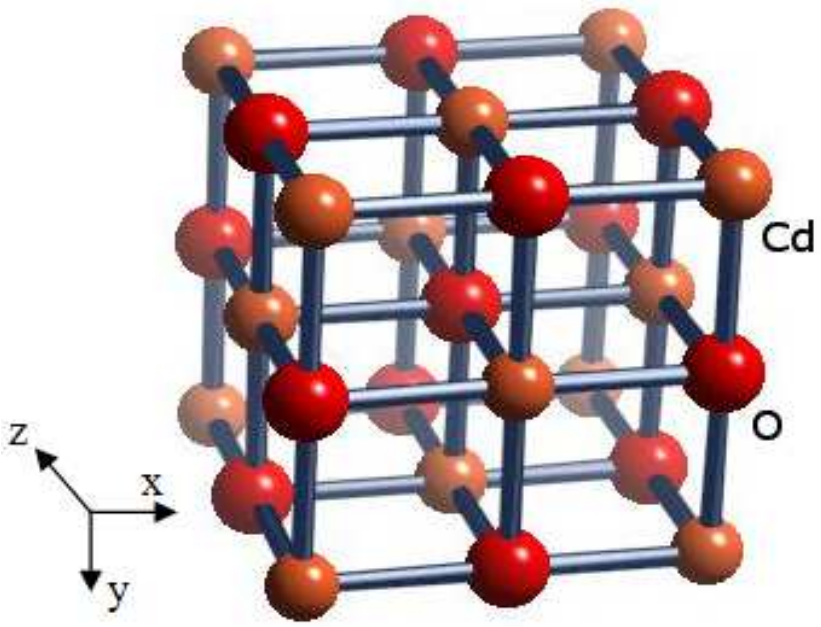

Figure 2.1: The crystal structure of CdO [64, 65].

2.7 Crystalline Structure of Semiconductors

Solids can be divided into two classes, namely, amorphous and crystalline. In an amorphous solid, atoms are not arranged in a long-range order. Thus, amorphous solids are also referred to as glassy solids. By contrast, a crystal is a solid formed by atoms [70]. Figure 2.2 shows that a lattice is an array of points in space that are arranged in a specific manner such that each point has identical surroundings. The smallest unit, which can be obtained by constructing planes through points called unit cell, and the lines resulting from the intersection of the planes at lattice points are known as lattice constants. As shown in Fig. 2.2, *a, b,* and *c* represent the lattice parameters. The shape and size of the lattice can be determined using the lattice constants values and the angles between the

lattice vectors. Thus, seven crystal systems are sufficient to cover all the 14 crystallographic possible lattices [70]. The crystal systems are divided into cubic, tetrahedral, hexagonal (or trigonal), orthorhombic, rhombohedral, monoclinic, and triclinic. Several of these systems can have different lattices, namely, simple or primitive (P), body centered (BC), and face centered (FC). CdO structured has face centered cubic type (FCC) [71].

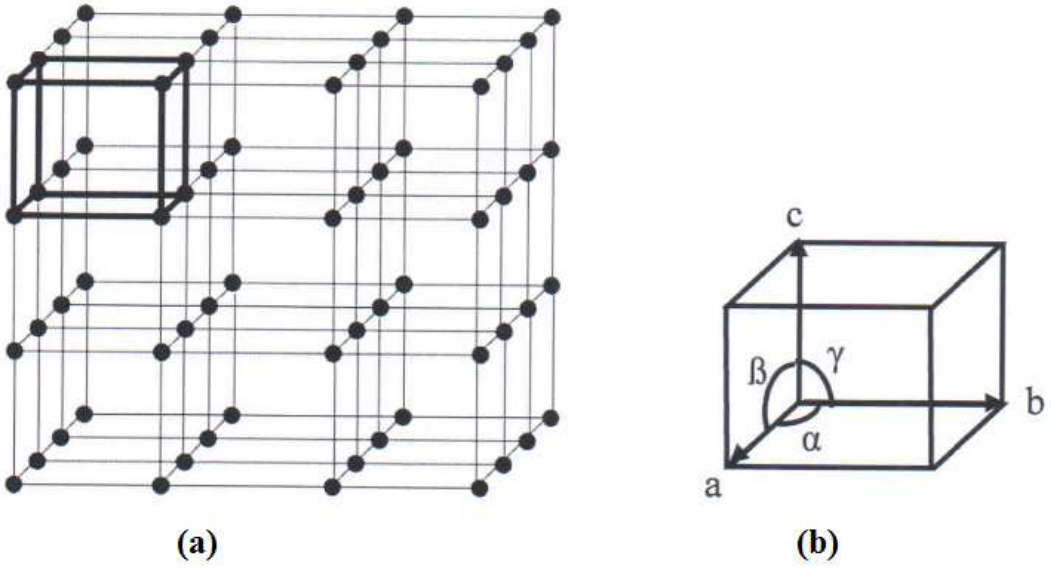

Figure 2.2: (a) Lattice, and (b) unit cell [71].

The CdO structure is a face centered cubic type (FCC), thus emphasis will be placed on the cubic system. The cubic system is the simplest crystal system where the three crystallographic vectors exhibit similar length and perpendicular to each other (a = b = c and $\alpha = \beta = \gamma = 90^{o}$). To describe the orientation of lattice planes, a set of three integers referred to as the Miller indices are used. Miller indices are the reciprocal intercepts of the plane on the unit cell axes. If the crystal plane makes fractional intercepts of (1/*h*), (1/*k*), and (1/*l*) with the three crystal axes, respectively, the Miller

indices are (*hkl*) [70]. Several lattice planes and their Miller indices in a unit cell with cubic structure are shown in Figure 2.3. The spacing between adjacent planes in a family is referred to as the *d-spacing*. The plane spacing formula of cubic structure is given by:

$$\frac{1}{d^2} = \frac{h^2 + k^2 + l^2}{a^2} \tag{2.1}$$

where a is the lattice constant. The crystalline structure of the materials can be examined using X-ray diffraction. X-ray pattern analysis is used to deduce the average crystallite size and the strain of the crystalline material.

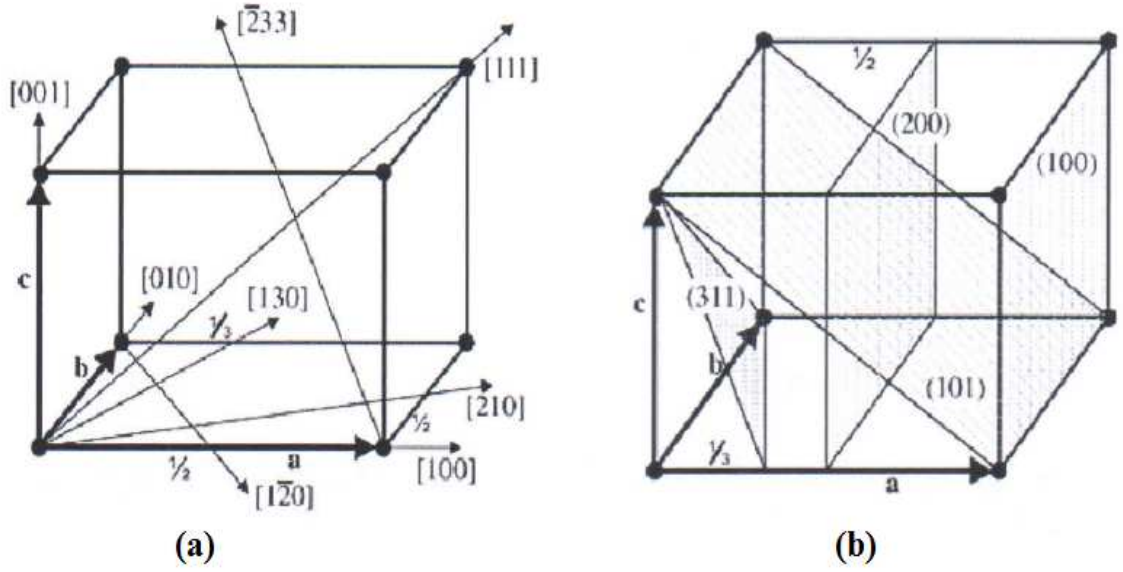

Figure 2.3: (a) Indices of lattice directions, and (b) Miller indices of lattice planes in cubic structure [70].

2.8 Band Theory in the Solid State

The band structure of a solid crystal is a very important factor with which to interpret electrical transport properties in solid-state materials. Every solid crystal contains carriers (electrons), which are organized in energy levels separated by energy

regions and do not have available wavelike electron orbits. Such a forbidden gap is called energy band gap (E_g), which is produced by the scattering of conduction electrons with the ion core of the solid crystal. The band structures of solid crystals can also classify solid-state materials into metal, semiconductor, and insulator, as shown in Figure 2.4. Solid crystals behave as metals if one or more bands are partially empty and partially filled regardless of temperature. Solid crystals are semiconductors if one or two bands are partially filled (the lower band regions known as valence band VB) or partially empty (the upper band regions known as conduction band CB). The forbidden energy regions that separate the valence and conduction bands are smaller in a semiconductor than in an insulator; thus, no electrons can move across this region in an electric field [72, 73].

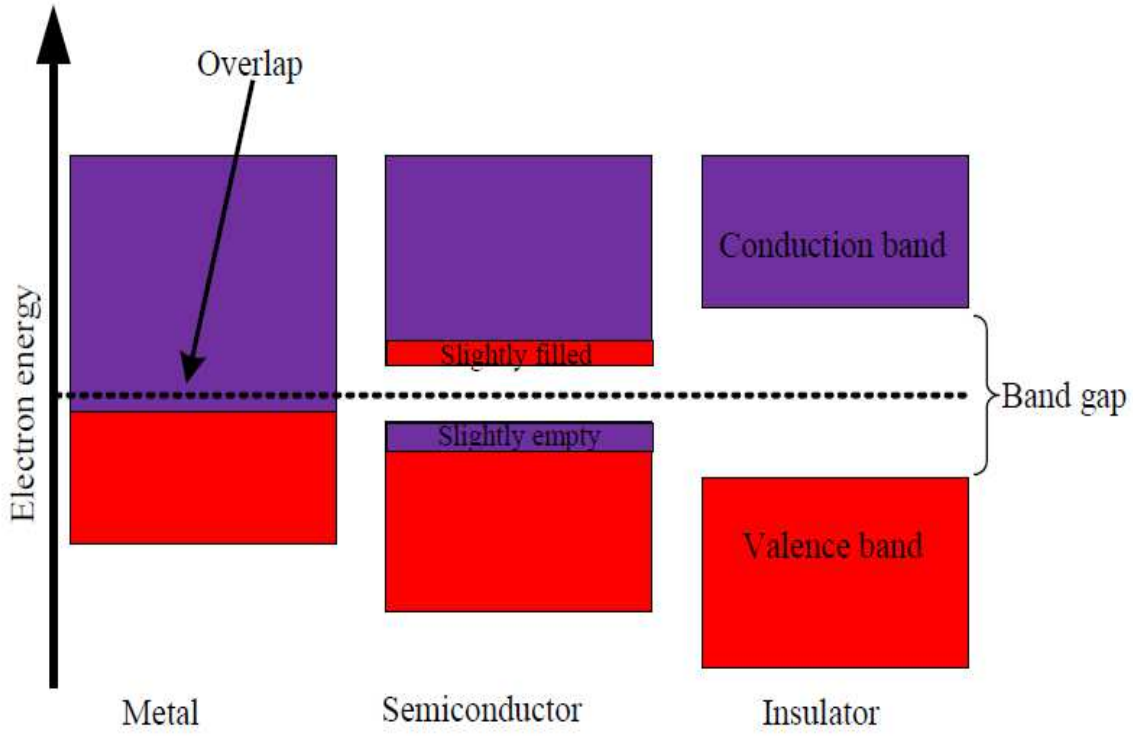

Figure 2.4: Diagram of the electronic band structure of metal, semiconductor, and insulator [72, 73].

2.9 Band Structure in Semiconductors

Semiconductors are characterized by their distinctive bonding types that include covalent bonding and ionic bonding. The energy band structures develop when atoms are sporadically set in semiconductor crystals [74]. The valence and conduction electrons communicate with the atoms in crystalline semiconductors, which slightly move the isolated energy intensity of the electrons to develop several energies with contrasting levels corresponding to the overall atomic numbers in the crystal. In order to ensure conductivity, electrons should exceed the amount of energy equivalent to the E_g:

$$E_g = E_C - E_V \tag{2.2}$$

where E_C is the lowest part of the conduction band energy level and E_V is the upper of the valence band energy level [74].

Semiconductors can be further divided into two groups: direct and indirect energy band gaps. The electrons present in semiconductors characterized with direct band gaps, can migrate from the valence band to the conduction band when their energy absorption is up to or greater than E_g, while the valence electron in the indirect band gap is incapable of migrating to the conduction band in the absence of phonon support, as shown in Figure 2.5 [74, 75]. The valence and conduction bands both comprise energy levels that can be packed with electrons or holes. The amount of these permissible states per unit of energy is referred to as density of state (DOS), and DOS for the electrons in the conduction band is represented as shown in equation 2.3 below:

$$N(E) = \frac{1}{2\pi^2 h^3}\left(2m_e^*\right)^{3/2}\left(E - E_g\right)^{1/2} \tag{2.3}$$

However DOS for the holes in the valence band is given by equation 2.4 shown below:

$$N(E) = \frac{1}{2\pi^2 h^3}\left(2m_h^*\right)^{3/2}(E)^{1/2} \tag{2.4}$$

where $N(E)$ is the DOS at energy E, m_e^*, m_h^* are the electron and effective hole masses, respectively, and h is Plank's constant. The probability of electrons absorbed in the electronic state in the conduction band is expressed by [71, 75]:

$$f(E) = \frac{1}{\exp\dfrac{(E - E_F)}{KT} + 1} \tag{2.5}$$

where E_F is the Fermi energy, K is Boltzmann's constant, T is the absolute temperature, and $f(E)$ represent the probability of finding the electron at energy E.

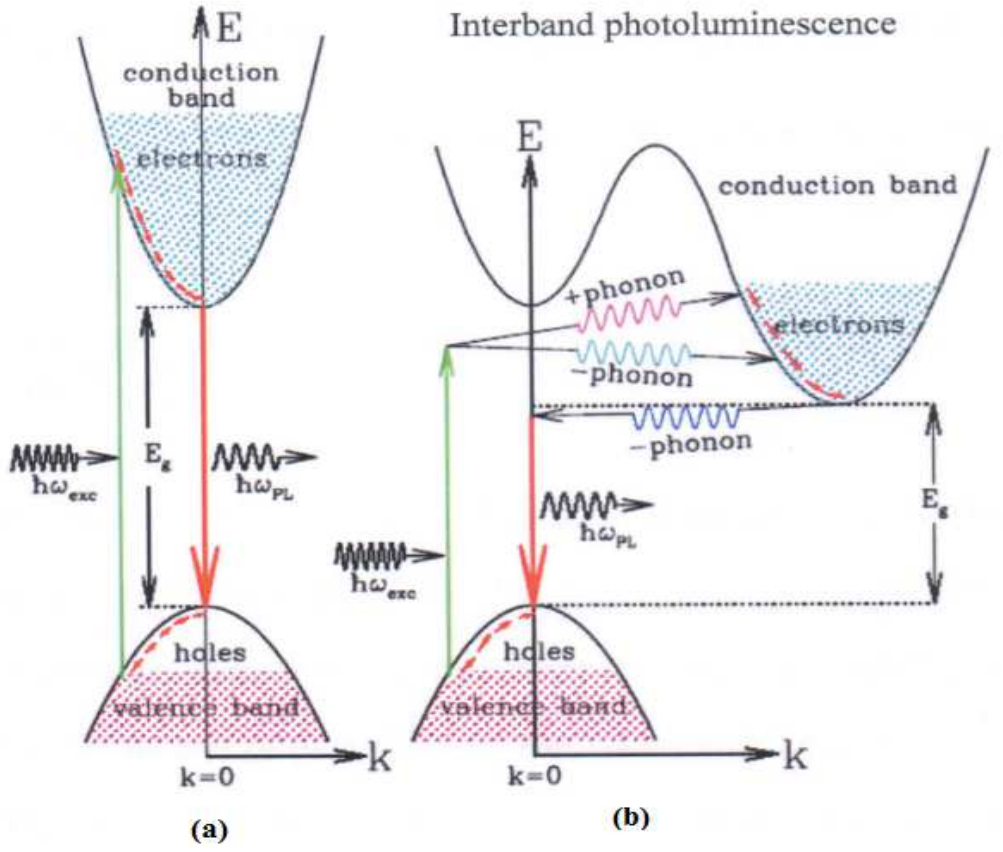

Figure 2.5: (a) Direct band gap, (b) indirect band gap [76].

The probability of holes occupying the electronic state in the valence band is giving by:

$$1 - f(E) = \frac{1}{\exp\frac{(E_F - E)}{KT} + 1} \tag{2.6}$$

Semiconductors are capable of a number of optical absorption, which include fundamental absorption, free carrier absorption, and energy level absorption within the band gap [74]. Fundamental absorption arises during the illumination of the semiconductor by a light with energy that exceeds that of the band gap, and excites the electrons in the valence band into the conduction band, thereby causing holes to be formed. In addition, other absorption types take place due to the amount of contamination in the band gap. In this absorption processes, the electrons transfer to another level of impurity, or from a donor level to the conduction band, or from valence to the accepter level, and so on. The absorption coefficient (α) represents the attenuation that occurs during the release of incident photon energy on the material as a result of the absorption processes. The Lambert relation between the absorption coefficient and the incident power intensity on thin films with thickness (*t*) is as follows [77, 78]:

$$I_{(t)} = I_o \exp[-\alpha t] \tag{2.7}$$

where $I_{(t)}$ is incident photon energy at thickness (*t*) inside the material, and I_o is incident photon energy at the surface of the material. The negative signal refers to the decreases in photon energy. The absorption coefficient is a function of the wavelength of incident radiation and it is very significant because it provides absorption range to the radiation. Absorption is derived from the following relation [77]:

$$A + R + T = 1 \tag{2.8}$$

where A is absorbance, R is reflectance, and T is transmittance.

When photon energy decreases to less than the energy gap; hence transmittance will be given as follows [79]:

$$T = (1-R)^2 e^{-\alpha t} \tag{2.9}$$

The relation between absorbance and transmittance is shown below [80]:

$$A = \log_{10}\left(1/T\right) \tag{2.10}$$

$$T = e^{-2.303\,A} \tag{2.11}$$

when T from Eq. (2.11) is substituted in Eq. (2.8), it results in:

$$e^{-2.303\,A} = (1-R)^2 e^{-\alpha t} \tag{2.12}$$

$$A = \left[\alpha t - 2\ell n(1-R)\right] / 2.303 \tag{2.13}$$

when R is very small ($R < 1$) then Eq. (2.12) becomes as follow [77]:

$$\alpha = 2.303 \times \frac{A}{t} \tag{2.14}$$

Transitions occur between the edges of the two bands (VB and CB) in semiconductor, which are described by Tauce formula [79, 81]:

$$\alpha h\nu = A(h\nu - E_g)^n \tag{2.15}$$

where A is a constant, $h\nu$ is the incident photon energy, and n is equal (1, 2/3, 1/2, 3/2) depending on the material and the type of the optical transitions (direct or indirect) [82]. The direct transition occurs between the top of VB and bottom of CB at the same wave vector $(\Delta K = 0)$. The allowed direct transition refers to that transition which occur between top of VB and the bottom of the CB when the change in the wave vector is zero

$(\Delta K = 0)$ and n = 1/2. For a number of semiconductor materials where the quantum selection system disallow the direct transition between the maximum of the VB and the minimum of CB, the transition occur at different positions of VB and CB (since $\Delta K = 0$). The transition is referred to as forbidden direct transition and n = 3/2, as shown in Figure 2.6 [74, 82].

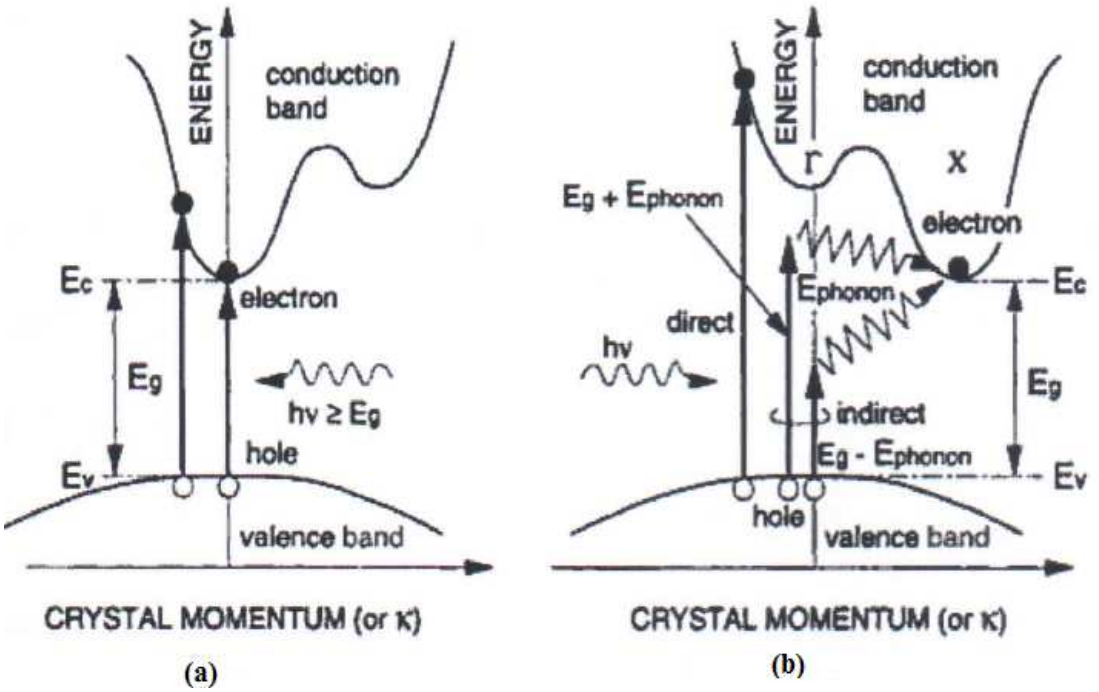

Figure 2.6: Absorption process in (a) direct band gap semiconductor, and (b) indirect band gap semiconductor [74].

On the other hand, the indirect transition takes place when the VB maximum and the CB minimum occur at different wave vector. Therefore, these transitions are limited by the low momentum conservation in crystalline semiconductors but unrestricted in amorphous semiconductors [73, 83]. Indirect transition involves the absorption or emission of phonons in order to stabilize the crystal momentum, as shown in Figure 2.6.

In this case the electron is unable to make a direct (perpendicular) transition from the VB to the CB except through a two-step process, because of variations in their crystal momentum. Therefore, the electron either absorbs both a photon and a phonon or absorbs a photon and emits a phonon simultaneously. The photon supplies the required energy while the phonon provides the needed momentum conservation [83].

2.10 Quantum Size Effects

The two basic factors that distinguish the behavior of nanocrystal from the corresponding macro crystalline materials depend on the size of individual nanocrystal. There is a high dispersity (large surface/volume ratio) associated with the particles, while the physical and chemical properties of the semiconductor are sensitive to the surface structure. Secondly, the actual size of the particle plays a significant role in determining the electronic and physical properties of the material. Reduction in size of the semiconductor crystal leads to the determination of Bohr radius, quantum confinement and the optoelectronic properties get modified [75].The electron and hole show more compaction in nanometer sized particles than in the macro crystalline material, and as a result there is a strong Coulomb interaction between electron and hole; they have higher kinetic energy than in the macro crystalline material.

The effect of three-dimensional confinement is that it collapses the continuous density of states of the bulk solid into the discrete electronic states of the nanocrystal. The finite size of the nanocrystal quantizes the allowed k values. Decreasing nanocrystal diameter shifts the first state to larger k values and increases the separation between states. Several models have been proposed to explain the dependence of exciton energy